SUPPLEMENTARY MATERIAL: UV-DIB: LABEL - FREE PERMEABILITY DETERMINATION USING DROPLET INTERFACE BILAYERS

Robert Strutt [1, 2] †, Felix Sheffield [1, 2] †, Nathan E. Barlow [1, 2], Anthony J. Flemming [4], John D. Harling [3], Robert V. Law [1, 2], Nicholas J. Brooks [1, 2], Laura M. C. Barter [1, 2] and Oscar Ces [1, 2] *

1 Department of Chemistry, Imperial College London, Molecular Sciences Research Hub, Shepherd's Bush, London, W12 0BZ, UK

2 Institute of Chemical Biology, Imperial College London, Molecular Sciences Research Hub, Shepherd's Bush, London, W12 0BZ, UK

3 Medicinal Chemistry, GlaxoSmithKline, Stevenage, SG1 2NY, UK

4 Syngenta, Jealott's Hill International Research Centre, Bracknell, Berkshire, RG42 6EY, UK

† These authors contributed equally. * Corresponding Authors.

Email: o.ces@imperial.ac.uk

DERIVATION FOR PERMEABILITY MODEL

Our permeability model is similar to one explored in Yohan Lee et al's cuvette based supported bilayer permeability system,[1,2] however adjustments were required for an equal volume system. Fick's first law[3] in the presence of a membrane was adjusted to an acceptor (C_A) / donor (C_D) model:

$$J = P\left(C_{D(t)} - C_{A(t)}\right) \qquad J = \frac{V_A}{A}\frac{dC_{A(t)}}{dt}$$

The assumption is made that flux is proportional to the concentration gradient (Fickian behavior). Secondly, that the volume of both droplets is constant across the course of the experiment, removing the need for a volume to be considered as a function of time. We used an initial concentration of permeant in $C_{D\,(0)}$. As shown by our leakage profiles the permeants do not leak into the oil phase and thus a mass balance which reflects this observation is:

$$C_{D(0)}V_D + C_{A(0)}V_A = C_{D(t)}V_D + C_{A(t)}V_A$$

Our experiments used an equal volume for both droplets where the error on pipetting volume is included in the downstream error propagation equation therefore: $V_D = V_A$. The equilibrium concentration is thus:

$$C_{EQ} = \frac{C_{D(t)} + C_{A(t)}}{2}$$

$$2C_{EQ} = C_{D(t)} + C_{A(t)}$$

Our central device records the acceptor compartment, which we consistently monitored across our experiments, droving out the $C_{D(t)}$ term gives equation 1.

$$\frac{dC_{A(t)}}{dt} = \frac{A}{V_A}\ 2P(C_{EQ} - C_{A(t)})$$

$$P = \frac{dC_{A(t)}}{dt}\frac{V_A}{2A\left(C_{EQ} - C_{A(t)}\right)}$$

Most data was fitted to equation 3 which is a derivation of the above equation for fitting to a concentration time curve, where P could be determined from the full permeability profile (scipy.optimizie.curve_fit and scipy.integrate.odeint). For the determination of the propagation of error equation, let:

$$m = \frac{dC_{A(t)}}{dt}$$

$$P = \frac{mV_A}{2A\left(C_{EQ} - C_{A(t)}\right)}$$

The partial derivative of each element:

$$\frac{\delta P}{\delta V_A} = \frac{m}{2A\left(C_{EQ} - C_{A(t)}\right)}$$

$$\frac{\delta P}{\delta A} = \frac{mV_A}{2A^2\left(C_{EQ} - C_{A(t)}\right)}$$

$$\frac{\delta P}{\delta C_A} = \frac{mV_A}{2A\left(C_{EQ} - C_{A(t)}\right)}$$

$$\frac{\delta P}{\delta m} = \frac{V_A}{2A\left(C_{EQ} - C_{A(t)}\right)}$$

Following the generic definition for error in a function:

$$f = XYZ$$

$$\delta f = f\sqrt{\left(\left(\frac{\delta X}{X}\right)^2 + \left(\frac{\delta Y}{Y}\right)^2 + \left(\frac{\delta Z}{Z}\right)^2\right)}$$

The propagated error equation for equation 1 is derived as:

$$\delta P = P\sqrt{\left(\left(\frac{\delta V_A}{V_A}\right)^2 + \left(\frac{\delta A}{A}\right)^2 + \left(\frac{\delta m}{m}\right)^2 + \left(\frac{\delta C_{A(t)}}{C_{EQ} - C_{A(t)}}\right)^2\right)}$$

Where δ indicates the standard error for each component.

BILAYER AREA DETERMINATION

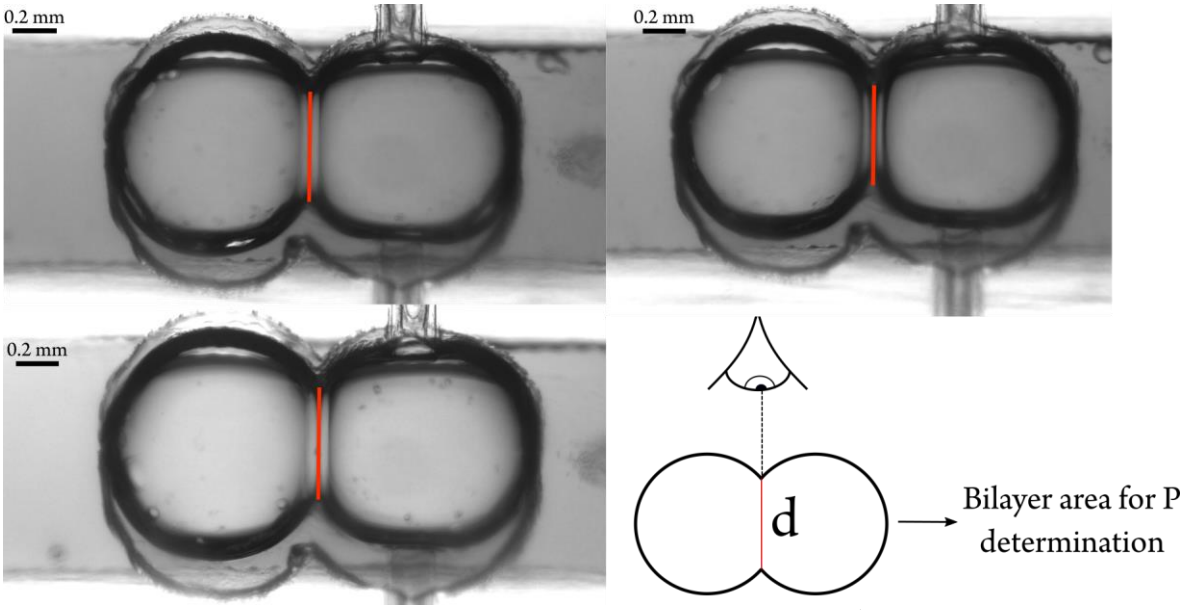

SUPPLEMENTARY FIGURE 1. Bilayer area assessment. DIBs were formed on-chip using 5 mg mL^{-1} lipid in the aqueous phase and 5 mg mL^{-1} lipid in the oil phase, these were subsequently imaged using standard light microscopy under 2X magnification. Images were captured 15 minutes after DIB formation to allow the droplets to arrive at an optimal morphology and equilibrium interfacial area. Images were processed using the ImageJ processing package to determine the diameter of the bilayer at equilibrium. This process was repeated for three individual DIBs to provide an average area and standard error of the mean to be fed into our propagated error equation shown previously. Assuming a circular geometry of the interface, the mean bilayer area was calculated which was then used to facilitate the determination of the membrane permeability. Error (SE) on this area measurement was fed into the propagation of error equation.

PROPOGATION OF ERROR STUDY

SUPPLEMENTARY TABLE 1: Summary of permeability experiments. SE calculated from the sample size reported next to the permeability value (Equation 1 and 3). Propagated error (Prop. Err.) derived above, P reported as the mean from each permeability coefficient (P). Lipids used: DOPC, 1,2-diphytanoyl-sn-glycero-3-phosphocholine (DPhPC), Soy Polar Lipid extract (SPLE). Green indicates that the SD from the permeability measurements is greater than the propagated error from the reported SE on independent measurements of the bilayer area.

Permeant	Lipid	DIB Formation Method	P ($x10^{-5}$ cm s^{-1})	SD ($x10^{-5}$ cm s^{-1})	SE ($x10^{-5}$ cm s^{-1})	Prop. Err. ($x10^{-5}$ cm s^{-1})
Caffeine	DOPC	In & Out	23.5 (8)	6.307	2.23	5.10
	DOPC	In	21.4 (3)	2.67	1.54	4.28
	DOPC	Out	28.1 (3)	1.59	0.92	2.95
	DPhPC	In	14.1 (3)	0.727	0.42	1.53
	SPLE	In & Out	14.9 (3)	1.80	1.04	1.70
Paracetamol	DOPC	In & Out	10.2 (8)	2.63	0.93	1.45
	DPhPC	In & Out	2.25 (3)	0.606	0.35	0.47
Thiamethoxam	DOPC	In & Out	14.5 (8)	2.46	0.87	1.49

For δV_A (±0.019 µL) the value was determined from the specifications of the utilized pipette. The change in concentration with time was determined within an appropriately linear region of a $C_{A(t)}$ vs t plot (R^2>0.95). δm, m and R^2 were calculated inside the employed least squares regression method (scipy.stats.linregress). This same method was used on the calibration curve to determine $\delta C_{A(t)}$, or the accuracy of converting from arbitrary units into concentration. We did not include the standard error for the individual points in the calibration curve although it is unlikely this will bare substantial influence on our final δP. We therefore deemed this method of characterizing the error within our system to be substantial. Due to the low volume and an estimation of the distance from membrane to optical path of ~ 200 µm, the diffusivity of the molecule was not considered.

Our analysis of permeability runs was performed using a python script and the integral intensity was converted into concentration via linear regression (y = mx +c). Our concentration vs time curves were normalized to the *apriori* known concentration of $C_{A(t=0)}$ and, following the observation of linearity, normalized to their independently observed equilibrium values following DIB rupture. Minor differences in intensity are reflected in the reported calibration curves SD for these concentration points. In the case of lipid in, vesicle size, where sample age directly correlates to the size of vesicle dispersion, could also affect this measurement. A further cause for this variance may also lie in the continuous use of the light source. In tandem we consider this a rigorous exploration of the sources of all error within our method and thus its applicability for use by other labs.

PYTHON SCRIPT LINEAR FIT PERMEABILITY ASSESSMENT RESULT WITH LINEAR FITTING

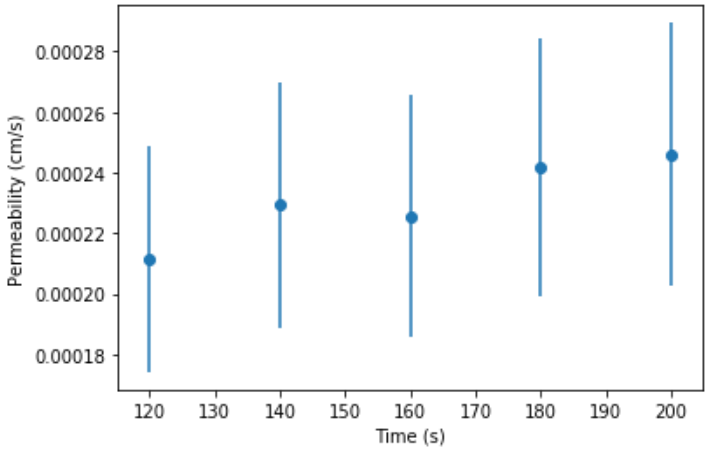

SUPPLEMNTARY FIGURE 2: Permeability assessment method. The permeability is calculated at each concentration point within a linear fit satisfying $R^2 > 0.95$, (here: $R^2 = 0.96$) within Fickian region of conc time curve (here: 120 – 200 s). Above shows result for experiment recorded with an interval of 20 s for a DOPC lipid in caffeine permeating system. Error bars show propagated error, the mean permeability (here: 23.8×10^{-5} cm s^{-1}) across this region is thus considered for each experiment and the SE within this mean added to the mean propagated error value for each time point (here: 5.12×10^{-5} cm s^{-1})

THEOPHYLLINE SYSTEM CONTROL FOR LEAKAGE

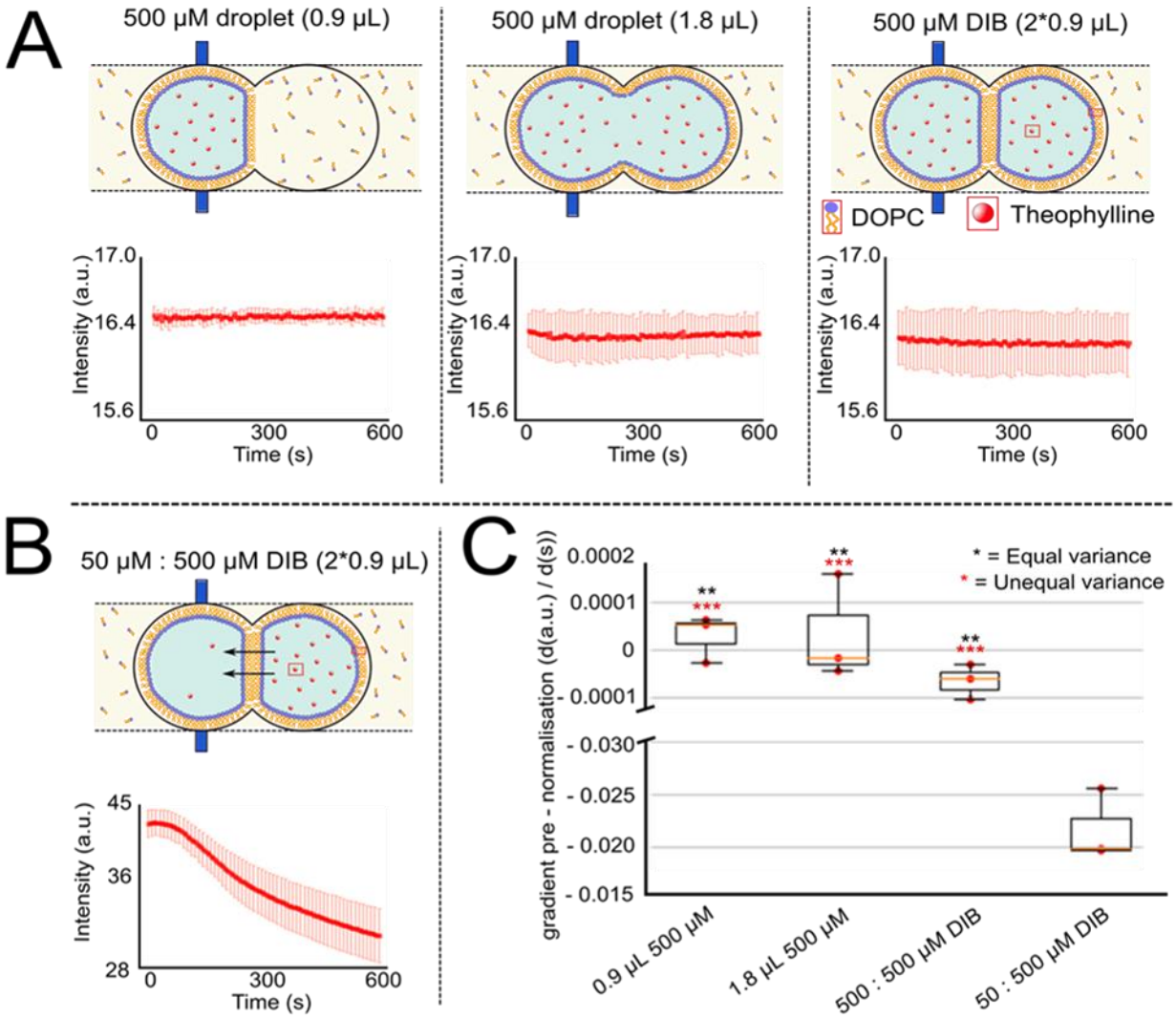

SUPPLEMENTARY FIGURE 3: A Calibration experiments show strong agreement in signal intensity for all possible system conformations for leakage studies. **B** Example permeation experiments show reduction in transmission intensity pre conversion to concentration. **C** Statistical testing of leakage to permeation data - a linear fit was performed to all time series to approximate the rate of change in transmittance. Fluctuation in the gradient around 0 was observed for all calibration experiments with an exclusively negative rate observed for all permeation experiments corresponding to acceptor concentration increasing in line with Fickian motion. Error bars represent 1SDOM, n=3 for all samples. Two tailed t-test comparing each calibration experiment (A) with permeability experiments (B) performed under the assumption of equal and unequal variance. *P < 0.05, **P < 0.01, ***P < 0.001.

THIAMETHOXAM AND CAFFEINE CALIBRATION / LEAKAGE DATA

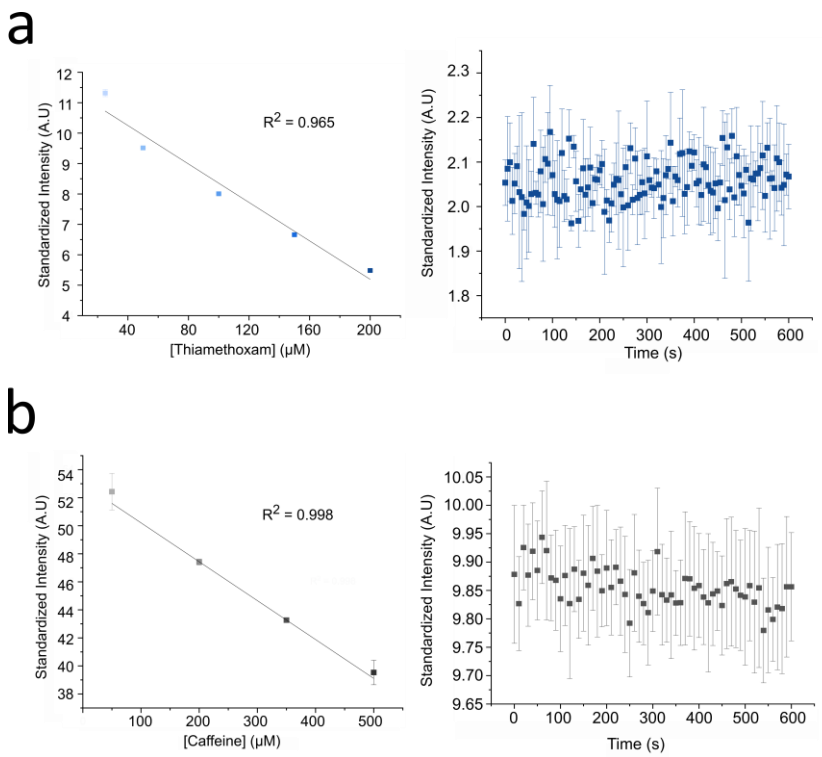

SUPPLEMENTARY FIGURE 4: Calibration and leakage data for both thiamethoxam and caffeine lipid in and out. Leakage assays were conducted so that n=3 for 600 s (SE shown for each data point), both leakage concentrations 500 μM and 5 mM respectively were outside of deemed linearity, when points were considered $R^2 = 0.9$ and 0.95 respectively. **a** Thiamethoxam calibration and leakage data. Intensity standardization was conducted for all experiments using the U and V ranges 250 – 275 nm and 350 – 375 nm respectively, where the spectra indicated maximal UV absorption in this U region. The use of a V range much closer to the U integration region was justified as it was determined that there was minimal absorption of UV light within this range as well as observing improved calibration linearity using this range. Lowest studied concentration of ~ 25 μM indicated LOD. Leakage assay show no significant flux into the oil phase. For DIBs established with concentration gradients, $C_{(t=o)DONOR} = 500$ and $C_{(t=o)ACCEPTOR} = 25$. **b** Caffeine calibration and leakage data. U and V ranges for all experiments of 270 – 290 and 450 – 550 nm respectively were used for intensity standardization. Leakage characterization was performed using 5 mM due to high solubility limit, indicating oil flux should not be significant at much lower concentrations. For DIBs established with concentration gradients, $C_{(t=o)DONOR} = 500$ and $C_{(t=o)ACCEPTOR} = 50$ μM.

.**THEOPHYLLINE IN AND OUT DATA**

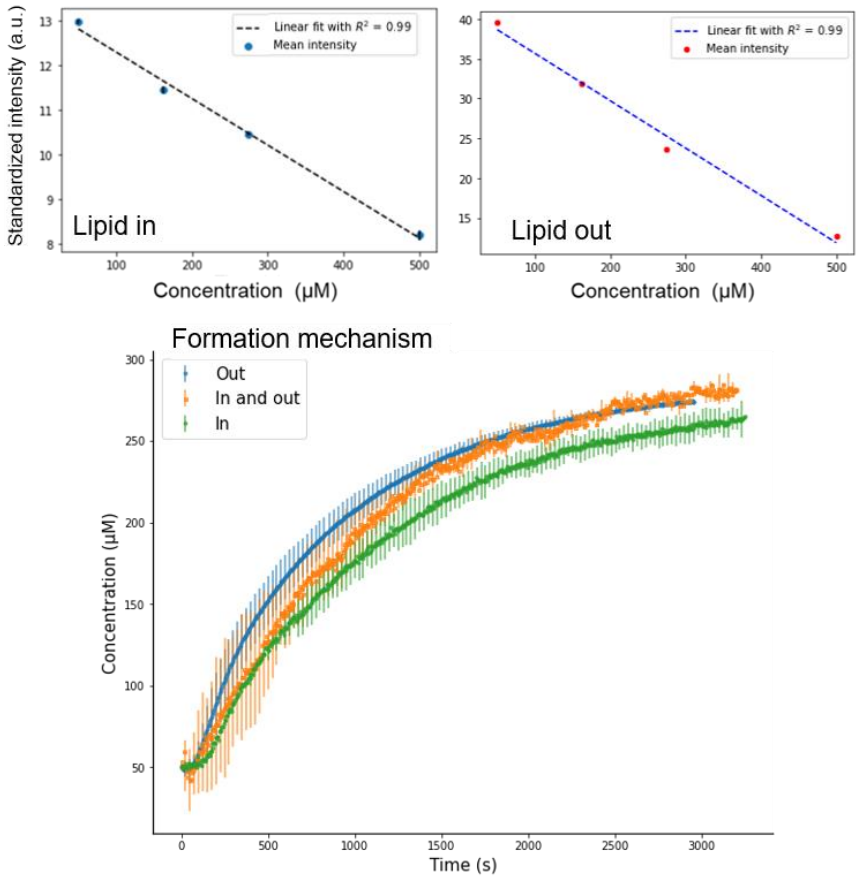

SUPPLEMNTARY FIGURE 5: Calibration data for Theophylline lipid in vs lipid out with linear region observed. Reduction in standard intensity across both methods attributed to light scattering in presence of vesicles. Concentration curves reflect rank ordering of permeability constants in figure 4. Interestingly it appears that the lipid in and out data (orange) is initially similar in rate to lipid in data (green) but equilibrates faster.

1-7 – DIMETHYLURIC ACID DATA

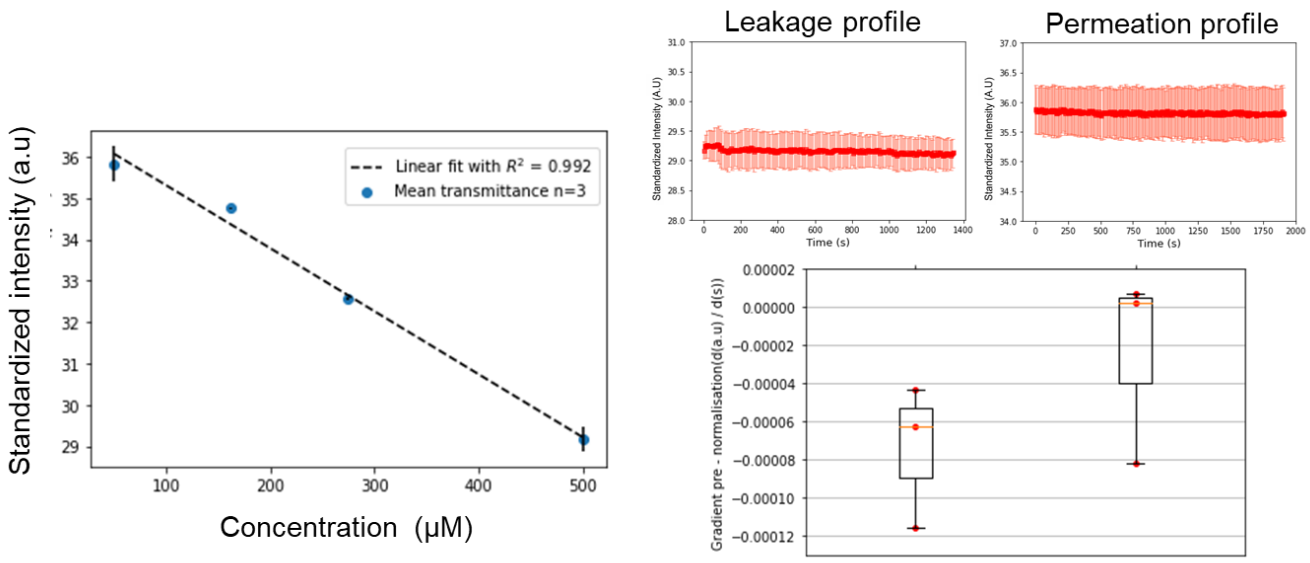

SUPPLEMENTARY FIGURE 6: 1-7 Dimethyluric acid is impermeable. Calibration shows expected linear region, lipid out DOPC. A linear fit of both leakage profile (performed with 500 uM 1.8 µL droplet), and permeation profile performed with an acceptor (50 µM) and donor (500 µM) shows no statistical difference between, a negative gradient in a permeation profile DIB would indicate permeation, however both profiles show a linear change in intensity with time. Gradient distributions attributed to noise / fluctuation in measurement.

CALIBRATION DATA FOR XANTHINE SERIES

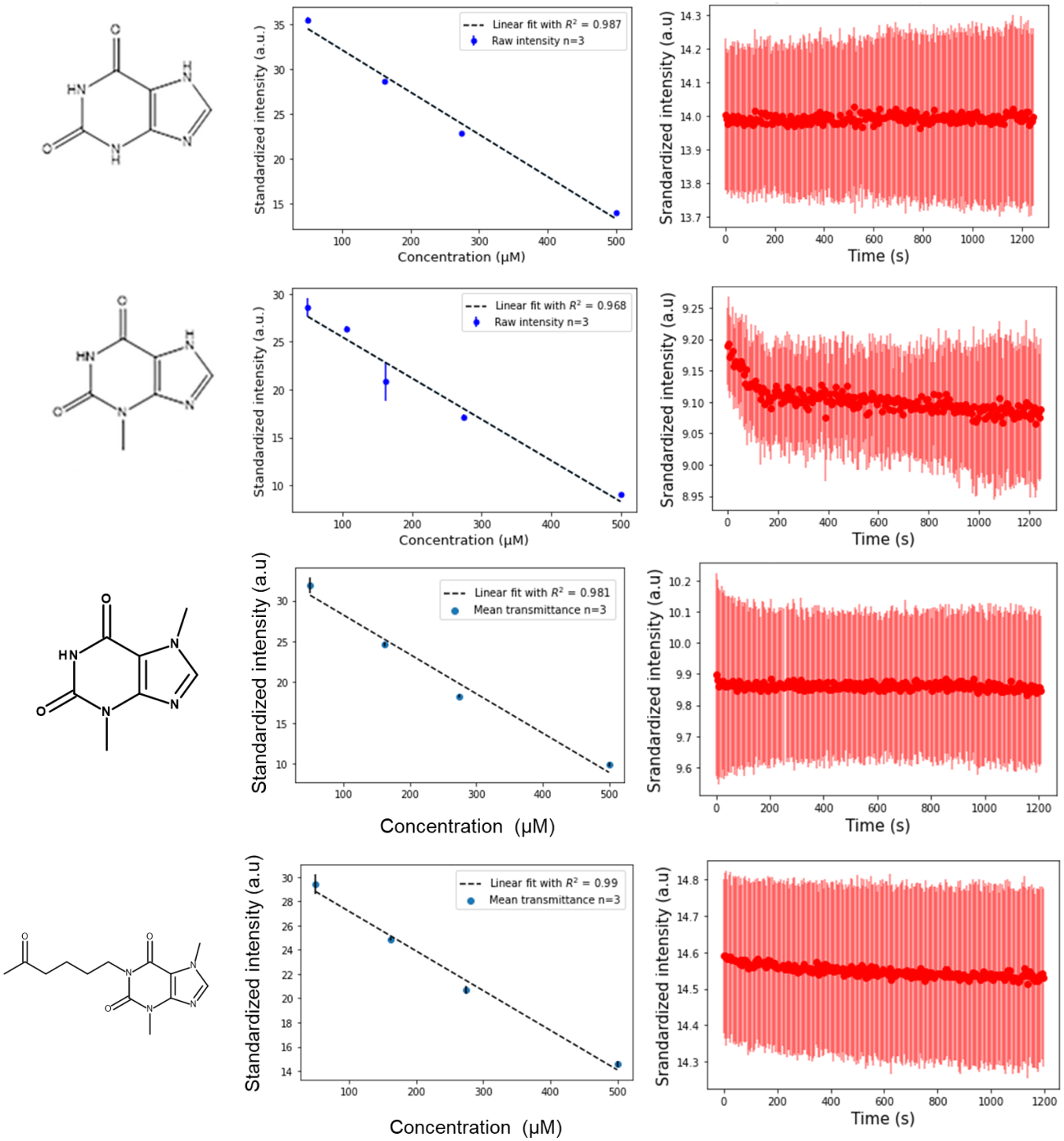

SUPPLEMENTARY FIGURE 7: Calibration data for xanthine series, all performed lipid out. Linear calibration observed for all compounds between 500 and 50 μM permitting donor and acceptor concentrations respectively. Leakage profiles of 500 uM, 1.8 μL droplets all indicate a flat distribution within a 1200 s window. Note that calibration data for theophylline, 1-7 dimethyluric acid and caffeine are featured in previous figures.

ALL TABULATED PERMEABILITY DATA

SUPPLEMENTARY TABLE 2: P calculated form at least 3 independent experiments. ALogP calculated with RDKit and AlogP calculated with Biovia draw software. HBA / D calculated with MarvinSketch.

Permeant	Lipid	Formation mechanism (Lipid)	Permeability ($x10^{-5}$ cm s^{-1}) (n)	SD ($x10^{-5}$ cm s^{-1})	MW (Da)	ALogP (RDkit)	ALogP (Marvin Sketch)	HBA/HBD	U/V regions (nm)	Conc A: Conc D (t=0) (uM)	Calibration - R^2
Caffeine	DOPC	In	21.4 (3)	2.67	194	-1.03	-0.0999	3/0	270-290 / 370 - 390	50 : 500	0.998
	DOPC	Out	28.1 (3)	1.59					270 – 290 / 450 - 550		0.985
	DOPC	In and out	23.5 (8)	6.307							0.998
	DPhPC	In	14.1 (3)	0.727							0.983
	DPhPC	Out	17.5 (3)	2.23					270-290 / 370 - 390		0.985
	SPLE	In and out	14.9 (3)	1.80					270 – 290 / 450 - 550		0.997
Xanthine	DOPC	Out	0.276 (5)	0.224	152	-1.06	-0.718	3/3	270 - 290 / 400 - 420	50 : 500	0.987
3-methylaxanthine	DOPC	Out	1.97 (3)	0.842	166	-1.05	-0.512	3/2	260-280 / 400 - 420	50 : 500	0.968
1-7 dimethyluric acid	DOPC	Out	Impermeable	n/a	196	-1.75	-1.35	5/4	260-280 / 400 - 420	50 : 500	0.992
Theophylline (0% DMSO)	DOPC	Out	19.4 (3)	2.35	180	-1.04	-0.305	3/1	260-280 / 350 - 390	50 : 500	0.990
		In and Out	15.0 (3)	2.26							
		In	13.7 (3)	1.82							
	DPhPC	Out	10.8 (3)	0.624							
Theophylline	DOPC	Out	18.2 (3)	0.923	180	-1.04	-0.305	3/1			

(1% DMSO)											
	DPhPC	Out	10.1 (3)	0.464							
Theophylline (3% DMSO)	DOPC	Out	17.4 (3)	0.377	180	-1.04	-0.305	3/1			
Theophylline (5 % DMSO)	DOPC	Out	15.0 (3)	2.48	180	-1.04	-0.305	3/1			
Theobromine	DOPC	Out	16.0 (3)	0.56	180	-1.04	-0.305	3/1	260-280 / 400 - 420	50 : 500	0.981
	DPhPC	Out	13.6 (3)	2.90							
Pentoxifylline	DOPC	Out	18.2 (3)	0.184	278	18	0.508	4/0	260-280 / 400 - 420	50 : 500	0.990
	DPhPC	Out	13.5 (3)	2.83							
Paracetamol	DOPC	Out	8.13 (3)	0.31	151	1.35	0.708	2/2	250 – 290 / 360 – 400	50:500	0.994
	DOPC	In and out	10.2 (8)	2.63					250 – 290 / 800 - 840	250:500	0.993
	DPhPC	In and out	2.25 (3)	0.606						100:500	0.982
	DPhPC	Out	3.34 (3)	0.726						50 : 500	0.994
Thiamethoxam	DOPC	Out	17.04 (8)	1.94	292	1.02	2.69	7/0	250 – 275/ 350 – 375	125:500	0.985
	DOPC	In and out	14.5 (8)	2.46						25:500	0.965
	SPLE	Out	14.60 (3)	1.06						50:500	0.983
	DPhPC	Out	6.25 (3)	0.57						50:500	0.986

THIAMETHOXAM DMSO EXPERIMENTS

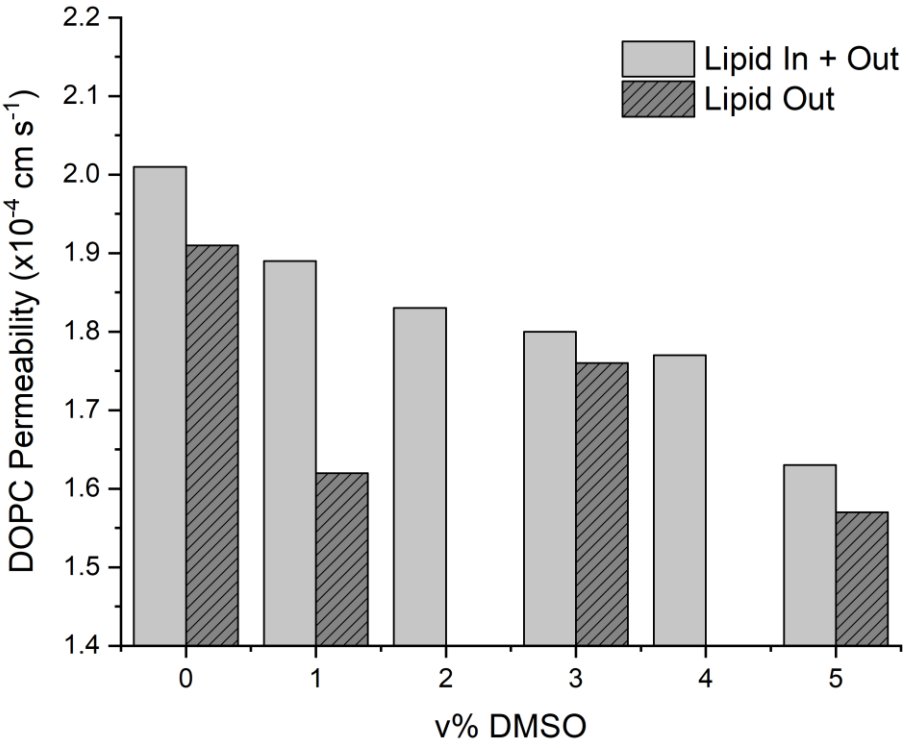

SUPPLEMENTARY FIGURE 8: Proof of concept experiments, probing the effect of DMSO concentration on the permeation rate of thiamethoxam. Each bar represents the permeability from an equilibrium permeation experiment where the permeability constant was derived by fitting the full concentration-time curve to equation 3 (n=1). In the cases of both DIB formation methods, lipid in and out as well as lipid out, a similar trend emerged where the permeability generally decreased with increasing DMSO concentration – as was found with theophylline.

SUPPLEMNTARY REFERENCES

1 Y. Lee, H.-R. Lee, K. Kim and S. Q. Choi, *Anal. Chem.*, 2018, **90**, 1660–1667.

2 Y. Lee and S. Q. Choi, *Eur. J. Pharm. Sci.*, 2019, **134**, 176–184.

3 A. Cass and A. Finkelstein, *J. Gen. Physiol.*, 1967, **50**, 1765–1784.